# ASPECTS ON CONCEPTUAL AND PRELIMINARY HELICOPTER DESIGN

A. Krenik, P. Weiand,
DLR Institute of Flight Systems, 38108 Braunschweig, Germany

**Abstract**

The German Aerospace Center (DLR) is currently developing a multidisciplinary design framework for conventional and unconventional rotorcraft. This program is the result of the project EDEN (Evaluation and DEsign of Novel rotorcraft concepts), which is a cooperation of the Institute for Flight Systems, the Institute for Aerodynamics and Flow Technology and the Institute of Structures and Design. The complexity of rotorcraft design requires the development of several subject-specific tools. Here, the components are continuously refined and published to the project group. This framework delivers a high level of modularity that makes the arrangement and testing of the process very flexible. The process starts with an empty workspace and the minimum input of payload mass, range, flight speed, number of rotor blades and a rotor configuration. The rotor configurations include also the unconventional types. The fundamental concept behind the layout of the tools inside the process is demonstrated especially the use of scaling and optimization loops. The implementation of more than one main rotor is in a special focus. Hence, the toolbox is dealing with different configurations and different mission requirements, the process itself can be called generic design.

## NOMENCLATURE

| | |
|---|---|
| $a$ | speed of sound, m/s |
| $c$ | chord, m |
| $\bar{c}$ | chord ratio |
| $c_T$ | rotor thrust coefficient |
| $c_{l\alpha}$ | lift curve slope |
| $d$ | foil thickness, m |
| $g$ | gravitational acceleration, $m/s^2$ |
| $l$ | rotor shaft spacing, m |
| $m$ | rotor disc area overlapping factor |
| $m_b$ | blade linear mass distribution, kg/m |
| $\hat{m}_f$ | fuel consumption, kg/km |
| $\dot{m}_f$ | fuel mass flow, kg/s |
| $s$ | thrust share coefficient |
| sfc | specific fuel consumption, $\mu$ g/J |
| $t_{flight}$ | endurance, min |
| $v_i$ | induced velocity, m/s |
| $w_d$ | descent speed, m/s |
| $E_{rot}$ | rotational energy of the rotor(s), J |
| $E_{trans}$ | translational energy of the helicopter, J |
| $I_b$ | moment of inertia of the blade, $kg/m^2$ |
| $M_f$ | fuel mass, kg |
| $M_p$ | payload mass, kg |
| $M_{OE}$ | operating empty mass, kg |
| $M_P$ | power source mass, kg |
| $M_{TO}$ | take-off mass, kg |
| $N_b$ | number of blades |
| $N_r$ | number of rotors |
| $P_{TO}$ | power at take-off mass, kW |
| $P_{ZF}$ | power at zero-fuel mass, kW |
| $R$ | range, km |
| $R$ | rotor radius, m |
| $U$ | blade tip speed, m/s |
| $V$ | air velocity, m/s |
| $V_{ground}$ | ground speed, m/s |
| $\gamma$ | Lock number |
| $\delta_b$ | relative foil thickness |
| $\varepsilon$ | energy ratio |
| $\kappa_{ov}$ | overlapping factor |
| $\mu$ | advance ratio |
| $\varrho$ | air density, $kg/m^3$ |
| $\varrho_b$ | blade mass density, $kg/m^3$ |
| $\sigma$ | rotor solidity |
| $\Omega$ | rotor frequency, rad/s |

## 1. INTRODUCTION

The design of rotorcraft is comparable to the design of fixed-wing aircraft, a highly multidisciplinary process. The technical layout and scaling of an aircraft with the respect to its Top Level Aircraft Requirements (TLARs) has a sustainable impact on the performance of the resulting configuration. Potential modifications in the design can, as later they occur, only be implemented with an increase of time and costs.

The basic performance of a design process is to concretize the information in order to increase the fidelity of the results with every step. In the standard references for aircraft design like Raymer [1] or Nicolai [2] the design process is divided into three main phases, the conceptual design, the preliminary design and the detailed design. Other references, like Layton [3] extend the three phases with a concept study at the beginning and a design proposal between the preliminary and the detailed phase.

In the 1980s and still in the 1990s there was the doctrine to freeze a design after every phase. Results of a previous design phases were not allowed to be changed in the following phases. With the introduction of computational multidisciplinary design processes the borders of the phases became blurred. If required tools can give a feedback to preceding tools, then the process has to be repeated to the originating tool.

The most crucial determination of the external configuration occurs at the end of the conceptual design phase. At this point the configuration and the major dimensions are defined. The most utilized rotorcraft configuration has one main rotor and one tail rotor to compensate for the main rotor torque. Furthermore, helicopter can have more than one main rotor (usually just two) being a representative of the so-called unconventional configurations. This includes only 4 different types: coaxial, intermeshing, side-by-side and tandem rotors arrangement, FIG 1.

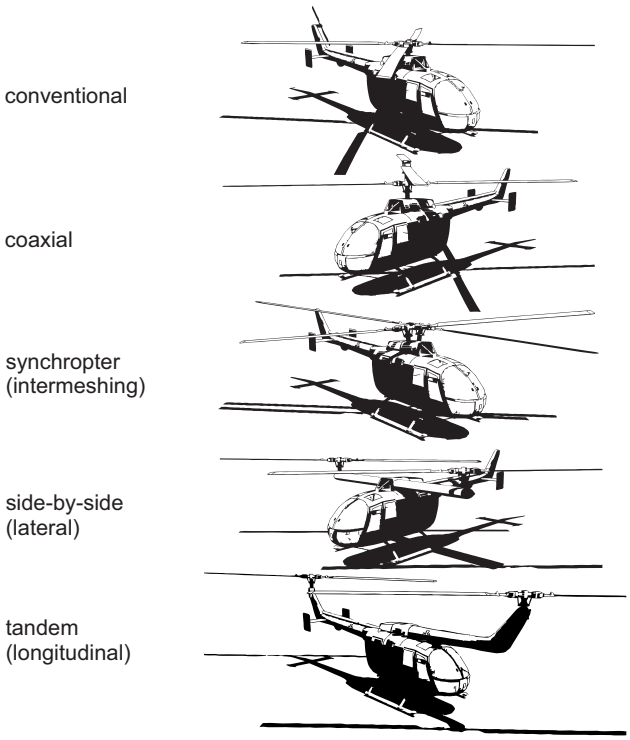


FIG 1. Different types of helicopters

According to Roskam [4] 65% of the final life cycle costs are determined after the end of the conceptual design phase. After the end of the preliminary design phase 85% of the upcoming costs cannot be influenced any more. Therefore the objective is a process chain that combines the tools of the conceptual phase and as far as possible the preliminary phase. Here, the methods used alternated between applying design tasks and analysis tasks. The essential performance is the functional arrangement of the tools according to their fidelity and computational time demand.

In resent years several aerospace research organizations presented approaches for multidisciplinary design processes in the field of rotorcraft engineering. Mentionable are the works of NASA [5], NLR [6], Georgia Tech [7] and ONERA [8]. In the last 10 years the German Aerospace Center developed design programs respectively process chains which dealt only with the design of fixed wing aircraft.

In 2011 the project RIDE[1] started to build up a process chain for Helicopter design. DLR internal project partners were the Institute of Flight Systems, the Institute of Aerodynamics and Flow Technology, both in Braunschweig, and the Institute of Structure and Design in Stuttgart. The objective was to build an integrated, automated and multidisciplinary design process, with only mission requirements, starting from scratch. The project had a strong focus on the development of a data set that allows a further processing of a rotorcraft design to high fidelity analysis and simulation methods in order to get information about the flight dynamics and flight properties of a virtual rotorcraft. In the process new calculation tools were developed as well as many tools from the fixed wing design were adapted to the boundary conditions of rotorcraft design. The conception behind these activities was to gather knowledge about the design process of rotorcraft and create a toolbox for generic and virtual design. In this project with a few exceptions the only configuration that was analysed was the classic configuration with one main and one tail rotor.

In 2014 the results and findings of project RIDE were processed into the new project EDEN[2]. Basic work packages of project EDEN are the further development of the process chain and the extension of the tools to novel respectively unconventional rotorcraft configurations. The design of a rotorcraft with more than one main rotor is an inherent capability of the toolbox. Here, the tandem rotors are partly overlapping and the coaxial rotors fully overlapping. By adding lifting surfaces and thrust producing elements like propellers or jet engines all helicopter types can be adapted to a compound configuration. The adequate calculation of the interferences of more than one main rotor and other compound elements is a continuing task in the EDEN project.

1 Rotorcraft Integrated Design an Evaluation

2 Evaluation and DEsign of Novel rotorcraft concepts

## 2. DESIGN LOOP AND INITIALIZATION

The design process loop starts with the so-called TLARs[3] consisting of only three parameters:

- cruising speed (not maximum speed)
- payload (which has to be transported at the defined cruising speed)
- range (which has to be fulfilled at the defined cruising speed, transporting the defined payload )

The initialization of the process creates the first dataset. The basis for this initial step is a statistical dataset of 159 existing helicopters, accumulated during the project RIDE. From here, all necessary parameters are evaluated to create an initial dataset, including the fuselage geometry choice and scaling.

Then, the created dataset is processed to a scaling loop. FIG 2 shows the basic layout. It iterates the maximum take of mass, which is the sum of the operating empty mass, payload mass and the fuel mass (1).

$$M_{TO} = M_{OE} + M_p + M_f \quad (1)$$

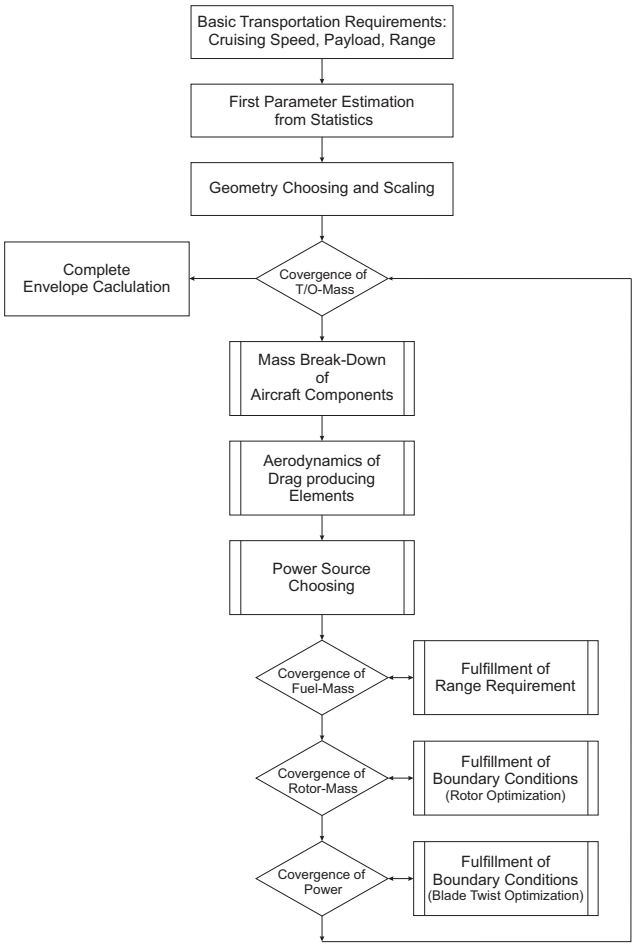


FIG 2. Flowchart of the design loop

Inside the loop the 1st station is the update of the operating empty mass by breaking it into component masses, such as structure, avionics, hydraulics, transmission, engine and so on. The 2nd station – aerodynamics – can be run through in parallel to the 1st, even though it is not the case in FIG 2, since there is no dependency between them. The 3rd station estimates engine power required, the engines' masses and the fuel consumption characteristics.

The 4th station is the 1st nested loop, in which the necessary amount of fuel referring to the TLARs and the chosen engine is calculated.

The 5th station is the 2nd nested loop dealing with the rotor parameter optimization, such as blade dimensions and blade loading.

The 6th station is the 3rd nested loop and optimizes the blade twist at the cruising speed for the minimum power requirement.

The design loop continues until significant changes in the take-off mass disappear.

At the end the converged design can be fed to the envelope calculation with a wide array of flight parameters.

Depending on the TLARs first dimensioning, both the three-dimensional expansion of the helicopter and the mass fractions are determined. FIG 3 shows a plot of the operating empty mass over the payload mass. In addition FIG 4 gives a plot of the fuel mass over the payload mass. In both cases the fractions of the take-off mass are parameterized by a potential approach. Depending on the primary design mission the variance in fuel mass to the best-fit curve can be moderate or high.

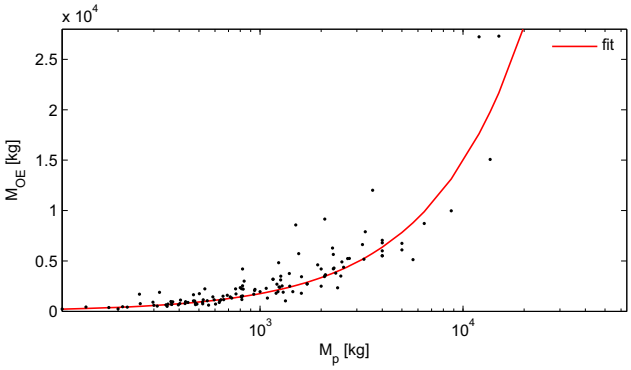


FIG 3. Statistical data of the operation empty mass over the payload mass with best-fit curve

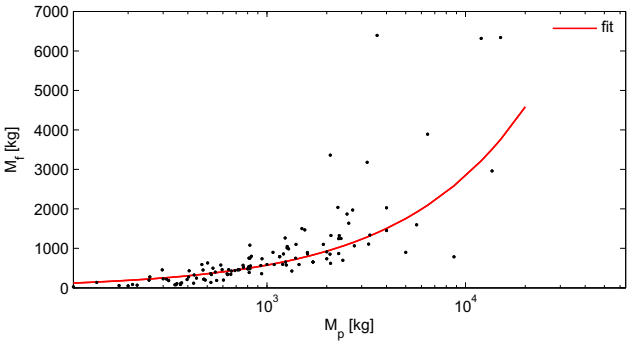


FIG 4. Statistical data of the fuel mass over the payload mass with a best-fit curve

Following the given TLARs the dimensions and positions of the rotors and the stabilizers are predicted for a desired configuration. In the data set, Rotor 1 is the main rotor for

[3] Top Level Aircraft Requirement

the standard configuration, the front rotor for the tandem or the upper rotor in case of the coaxial configuration, left for the synchropter and side-by-side configuration. Rotor 2 is consequently the tail rotor, rear rotor, lower rotor or right rotor. Every design approach considers right from the beginning at least two rotors. Other compensations for main rotor torque, like NOTAR or Fenestron are not included for now.

The size of the fuselage, respectively the body is derived from the required cabin volume. A generic fuselage is scaled according to the required cabin. The fuselage is arranged under the rotors with the centre of the payload mass in the centre of gravity of the configuration. The fuselage body can be separated into “FuselageFront” with cockpit and the avionics, the “FuselageMid” with the cabin and the “FuselageRear” with a possible ramp or a cargo hold. FIG 5 shows the arrangement of the components and the component parts. The dimensions of the front and rear fuselage body are at minimum derived by standard aspect ratios but vary by adding requirements for retractable nose gears or enhanced avionics at the front or special loading characteristics at the stern ramp.

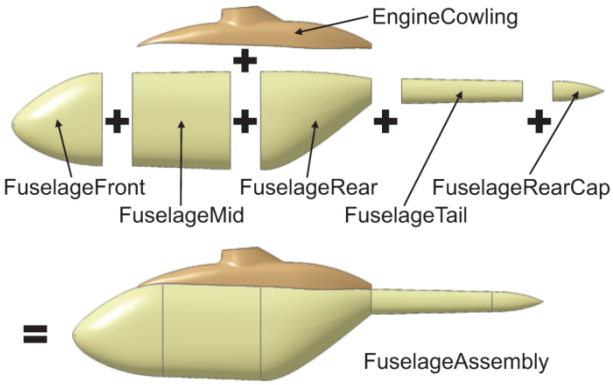


FIG 5. Component parts and assembly of the generic fuselage approach

While the scaling of the rotors is related to the maximum take of mass, the fuselage is scaled from the payload volume. The correlation of the regression curve and the statics, presented in FIG 6 is very good. By including other geometric ratios the prediction of an average cabin shape from the take-off mass gives reasonable initial results.

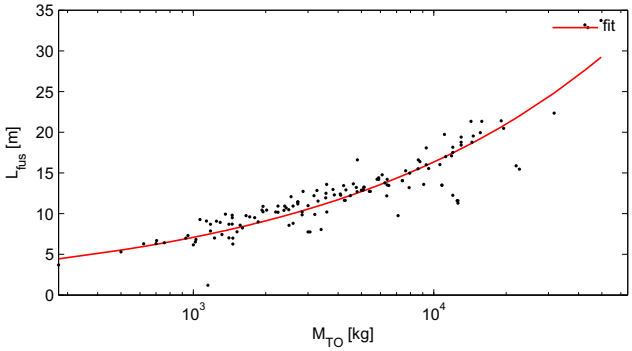


FIG 6. Statistical data of the fuselage length over the maximum take-off mass with a regression curve

## 3. ITERATIVE PROCESSING AND OPTIMIZATION

The design loop and the optimization algorithms are implemented within the distributed, workflow-driven integration environment RCE[4], developed by DLR.

### 3.1. Mass Estimation of Components

The more sophisticated prediction of the operating empty mass is conducted by calculating the masses of the several components. Therefore formulas by Beltramo [9], Layton [3] and Prouty [10] are available. In addition Palasis [11] has already analyzed a combination of the formulas by Beltramo and Layton. The weight models of the AFDD (Aero Flight Dynamics Directorate) presented by Johnson [5] are most recent and have highest coupling between geometric and performance parameters with the respective component weight. Small changes in the geometrical dimensions result in recognizable changes of the empty mass. Consequently the size of the rotors and the required installed power is scaled with the take-off mass. A best of combination of the available models is still in progress.

After calculating the updated maximum take-off mass a convergence check is conducted. The data set is iterated until mass, size and flight performance is consistent and the loop is converged. Iterations to minimize deviation below 1% of the take-off mass are not reasonable since the accuracy of the utilized tools is recognizable lower. The framework software needs an additional feedback from all nested loops to insure they have finished their computation before. In total three nested loops were used inside the outer scaling loop. The previous initialization and the subsequent calculation of the flight envelope are arranged straight forward, see FIG 2.

### 3.2. Fuselage Aerodynamics

From the adapted external configuration a 3D-model is created according to FIG 5. The approach based on the work of Kunze [12] then calculates the aerodynamic properties of the specific 3D-model by the use of a modified version of VSAERO [13]. The program uses a linearized 3D-panel-method with a coupled viscous solver. FIG 7 shows the pressure distribution on the surface of a fuselage up to the separation line. In general the helicopter fuselage has a region of separated flow on the backside below the tail boom, due to its blunt shape. Vortexes of separated flow strongly increase the parasite drag reducing the flight performance in terms of increasing the required power. Therefore flow separation has to be taken into account. The automated modelling of the streamlines by the use of wake panels showed to be problematic and less robust. Another method is to assume a constant pressure on the surface panels with separated flow. The line of separation is predicted by boundary layer code integrated into VSAERO. The value for the pressure coefficient behind the separation line can be calculated or manually set. The calculation of the clean fuselage surface is extended by some handbook methods to take additional parts like the rotor hub, landing gears and more into account. The aerodynamic drag is the basis for the flight performance calculation.

[4] Remote Component Environment

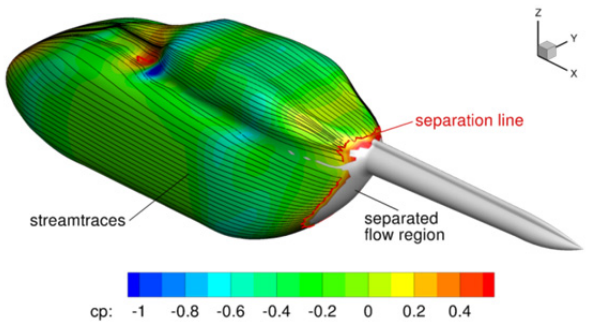


FIG 7. Results of the calculation of the pressure distribution on the helicopter fuselage

### 3.3. Rotary Wing Aircraft Calulations

All required flight mechanics calculations within the design loop are performed by the Helicopter Overall Simulation Tool (HOST). The word tool at the end of the acronym is a clear understatement, because the code behind it can be considered as a full-fledged virtual rotorcraft design and evaluation operating system. The addressed functions of HOST in the process chain are only a fraction of its possibilities. The main task here is to perform trim calculations referring to the TLARs with continuously varying datasets. The main output is the required power consumption.

The special nature of all multiple main rotor configurations is the existence of mutual rotor-rotor interactions, which are most pronounced at hover and low flight speeds. For this reason models of super positioned induced velocity fields were developed and applied with HOST. The basic approach is to perform one calculation without mutual rotor interactions and to use the results to shape the additional velocity field as an overlay and to perform a second trim calculation with the synthesized overlay. The factors for the induced velocity increase were derived from Johnson [16]. FIG 8 and FIG 9 show the induced velocities at hover and in forward flight for a coaxial and a tandem configuration after (double) trim calculations.

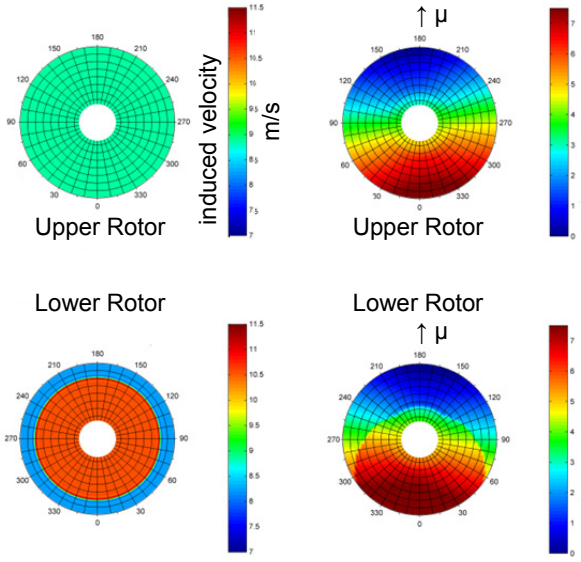


FIG 8. Resulting induced velocity fields in hover (left) and forward flight (right) at Ω=424 rpm, μ=0.08, 2.2 tons take-off mass for the coaxial rotor arrangement

In the hover case of the coaxial arrangement the lower rotor is highly affected by the contracted downwash of the upper rotor as can be seen as a concentric disc of 90% of the radius. In forward flight the downwash of the upper rotor is swept back downstream, reducing the affected area of the lower rotor disc. In the hover case of the tandem arrangement (FIG 9) the fore rotor is highly affected by the downwash of the aft rotor, as the aft rotor is above the fore rotor. In forward flight the intermeshing area shrinks due to downstream inclination of both rotor wakes – in principle due to the same reasons as with the coaxial type.

The impact on power consumption compared to the in reality non-existing but calculated case of non-interacting treatment of the rotors is shown in FIG 10. The increased power consumption is highest at hover decreasing almost to negligible values at cruising speed. To take the rotor head penalty into account each rotor shaft is modeled as a cylinder in a flow and the rotor blade area between the rotor shaft and the aerodynamic beginning (beginning of the airfoil) is modeled as a 2-dimensional drag producing cylinder section.

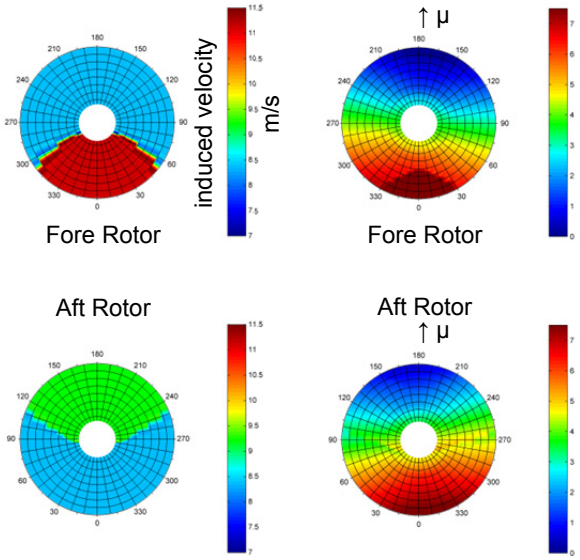


FIG 9. Resulting induced velocity fields in hover (left) and forward flight (right) at Ω=424 rpm, μ=0.08, 2.2 tons take-off mass for the tandem rotor arrangement

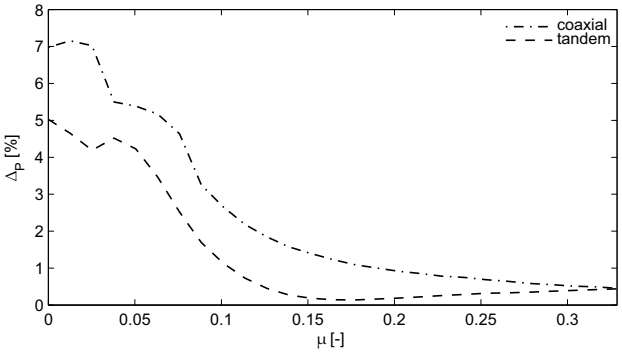


FIG 10. Increase of power consumption due to mutual rotor interactions, relative to the non-interacting case

### 3.4. Estimation of Engine Mass and Fuel Consumption

The adequate choice of the power source within the iterative preliminary design loop is not a matter of browsing a catalogue of available engines. Instead the evaluation of the engines database is paired with the database of the helicopters. The ratio of the overall engine's mass related to the maximum take-off mass of each helicopter from the paired databases is shown in FIG 11.

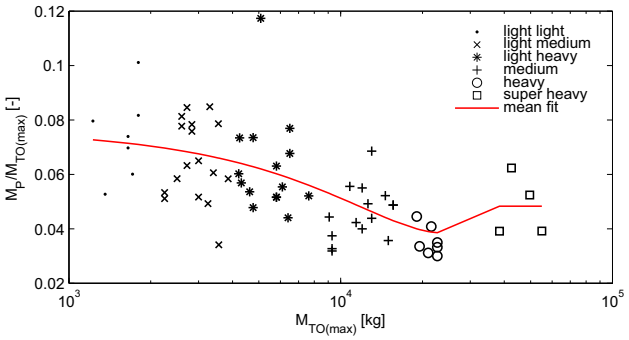


FIG 11. Fraction of the installed power mass related to the maximum take-off mass

The helicopters were subdivided into 6 weight classes, starting with the maximum value of 2 tons for the "light-light", doubling the maximum value for each following higher class up to the "super-heavy" (maximum of 64 tons). For each weight class the data was averaged and a fit-function was applied.

It can be seen that the mean fraction of the installed power mass related to the maximum take-off mass decreases throughout the first 5 weight classes, just slightly increasing at the few realized "super-heavy" helicopters. The explanation for this trend might be the circumstance that in general the effectiveness of the shaft-turbine engines increases with the overall size, also conditioned with the technological issue of more experience with the lighter weight classes, in contrast to the older few individuals of the "super-heavy" class.

The same procedure as before was applied for the estimation of the specific fuel consumption at take-off power setting (FIG 12). The trend here is almost the same as with the engine's masses.

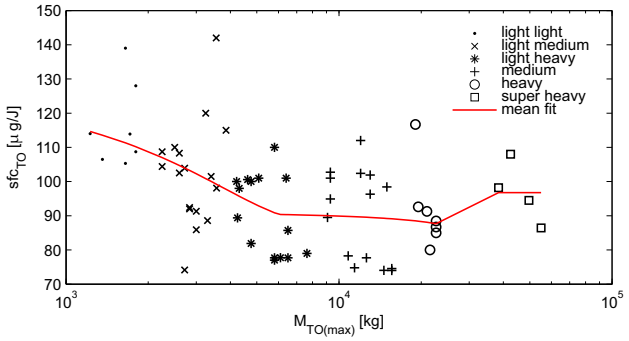


FIG 12. Specific fuel consumption at take-off power setting

The specific fuel consumption for the continuous power regimes is in most cases 8 to 9% higher than that of the take-off regime. So the values of the fit-functions are multiplied with the factor of 1.1 for the endurance and range calculation. With this approach there is no need to estimate the absolute required power for the concerning flight regimes of the preliminarily designed helicopter.

### 3.5. Endurance and Range Calculation

At this point of the design loop the dataset of the helicopter is defined. Now, the flight mechanics characteristics at steady flight conditions – to be fulfilled as set up from the basic requirements – like cruising speed with the defined payload and range at cruising speed can be calculated.

For that purpose the endurance and consequently the range calculation can be easily performed and furthermore the required fuel mass can be accurately determined, in contrast to the roughly estimated amount before (shown in FIG 4).

The endurance calculation is accomplished with the so-called "mean fuel flow"-method, which was found to be very accurate throughout the velocity envelope, requiring only 2 trim-calculations (1. with a full fuel tank and 2. with zero fuel mass) for each flight regime. The mean fuel flow is:

$$\bar{\dot{m}}_f = \frac{1}{2}\left(\dot{m}_{f\,(TO)} + \dot{m}_{f\,(ZF)}\right) = \frac{1}{2}\left(\begin{array}{l} f_{engine}\left(P_{TO}\left(M_{TO}\right)\right) + \\ f_{engine}\left(P_{ZF}\left(M_{ZF} = M_{TO} - M_f\right)\right) \end{array}\right) \quad (2)$$

The resulting flight duration then is simply:

$$t_{flight} = \frac{M_f}{\bar{\dot{m}}_f} \quad (3)$$

The range is calculated as follows:

$$R = V_{ground} \cdot t_{flight} \quad (4)$$

With this output the required fuel mass can be found by application of an iterating and converging loop with the following formulation at which the following outputs from HOST trim-calculations have to converge:

$$Outputs_{HOST} : \begin{cases} M_{f,old} \\ R_{actual} \\ R_{required} \end{cases}$$

The difference of the actual and required range is calculated in the iteration loop:

$$\Delta R = R_{actual} - R_{requiered} \quad (5)$$

The average fuel consumption per unit flight range is:

$$\hat{m}_f = M_{f,old} / R_{actual} \quad (6)$$

The improved fuel mass setting for the required range from (5) and (6) then is:

$$M_{f,new} = M_{f,old} - \hat{m}_f \cdot \Delta R \quad (7)$$

The new fuel mass is then handed over into the trim-calculation from the beginning of the loop. Mostly it takes 3 iterations to fulfill the requirement (in terms of calculated range) with a deviation of less than 2 km.

At that point the fuel tank is exactly filled and the overall mass is (in most cases) reduced, compared to the estimation from the initiation, based on statistics.

The next step in the loop is the rotor parameter determination to fulfill the set up boundary conditions and in general to optimize them in terms of one or more selected criteria.

### 3.6. Rotor Parameter Optimization

The rotor parameter optimization follows the “call and response”-approach, meaning that there are only three parameters of the rotor which are the calling inputs (number of blades is set and the rotor blade twist is considered later in the design loop):

- rotor blade chord
- rotor blade length
- rotational frequency of the rotor

On the other side the dependent functions from inputs serve as responses. For that purpose the module ParRot[5] was developed and coupled with the optimization algorithm COBYLA[6] [14]. The optimization goal is to achieve the lightest rotor blade.

#### 3.6.1. Design Parameters (inputs)

The main three rotor design parameters are initially set from the evaluation of the statistical database and their lower and upper boundaries form the permitted design space for iterative optimization process. In the following the design input parameters extracted from the database are presented.

- **Chord**

The chord (FIG 13) has a slightly degressive trend (even though the logarithmic scaling distorts it to the opposite) from the database.

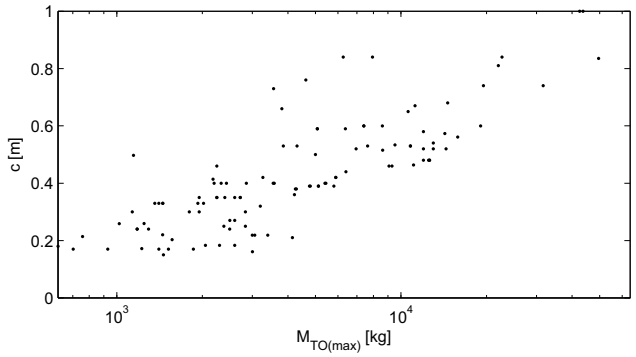


FIG 13. Chord from helicopter database

- **Radius**

The rotor radius (FIG 14) follows a more precise trend than the chord, but also degressive with increasing take-off mass.

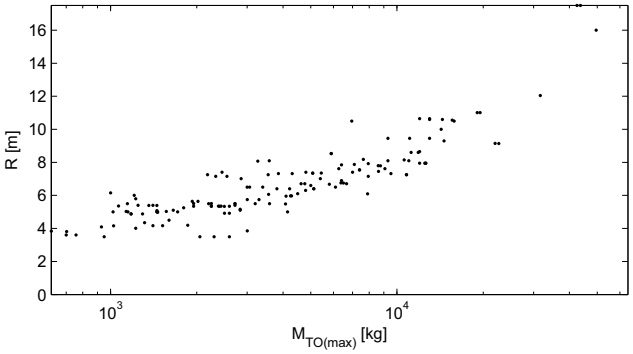


FIG 14. Rotor radius from helicopter database

- **Rotor Speed**

The rotational frequency or rotor speed (FIG 15) of the rotor has reciprocal relation to the rotor radius, as the tip speed is mostly set within a relative thin margin:

(8) $$\Omega = \frac{U}{R}$$

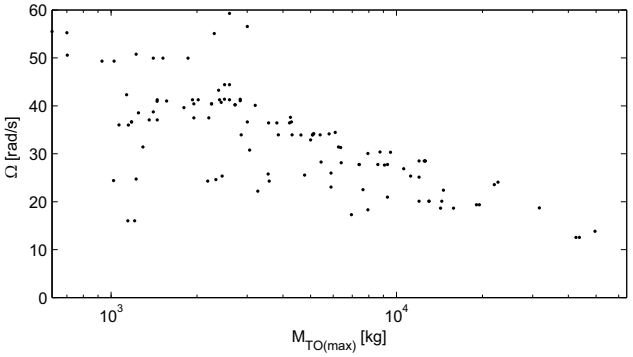


FIG 15. Rotational frequency of rotors from helicopter database

- **Number of Blades**

The only parameter, which is not varied throughout the design and optimization loop is the number of rotor blades per rotor, because of the natural number type, which is not suitable for most of the optimization algorithms and because it is a matter of preferences, as can be seen in FIG 16. The simplest rotor of two blades was used for take-off masses of up to 8 tons (Bell 214-ST). The widest range have the 3-bladed rotors with take-off masses of up to 13 tons (with coaxial rotors of the Ka-27). The single rotors end at 3.6 tons of the S-62. The 3-bladed rotor is preferred by all tandem configurations and (except for the X² and S-97 from Sikorsky) is still standard to the coaxial configurations among Kamov’s designs. It can be said that any number of blades between 2 and 4 can be chosen in the weight category between 1 and 10 tons. Above that 5 to 8 should be preferred.

[5] Parametrization of the Rotor
[6] Constrained Optimization BY Linear Approximation

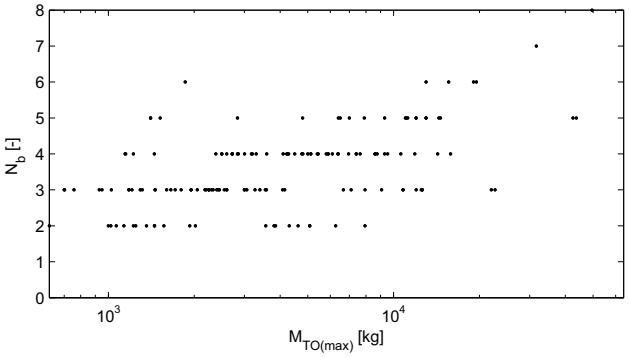


FIG 16. Number of blades per rotor from helicopter database

So, on the one hand there are three parameters of the rotor, which are to be found optimal for a specified flight condition (or design point) and on the other hand there are (some) rival and conflicting parameters (among those the inputs themselves), which are constricted by boundary conditions with the aim of receiving only one solution. This is true for example for the rotor length and the rotor frequency in terms of blade tip speed.

### 3.6.2. Design Characteristics (outputs)

The design characteristics from the variation of the afore mentioned parameters, or in that case - responses, are described in the following.

- **Chord Ratio**

The ratio of the blade chord to the blade radius

(9) $$\bar{c} = c/R$$

has no recognizable trend, hence can be treated as a constant bandwidth throughout the whole database, as can be seen in FIG 17. So the boundary conditions can be roughly set to 0.04 and 0.08.

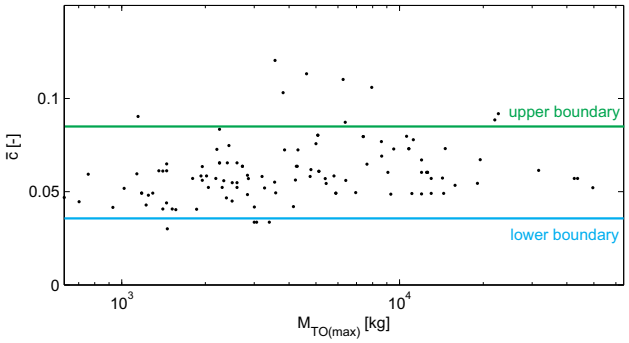


FIG 17. Chord ratio from helicopter database

- **Rotor Solidity**

The rotor solidity is the ratio of all blade planforms related to the rotor disc area:

(10) $$\sigma = \frac{N_b\, c\, R}{\pi\, R^2} = \frac{N_b\, c}{\pi\, R}$$

It has a degressive increase with the take-off mass as can be seen in FIG 18. In general the boundary conditions can be set to 0.03 and 0.12.

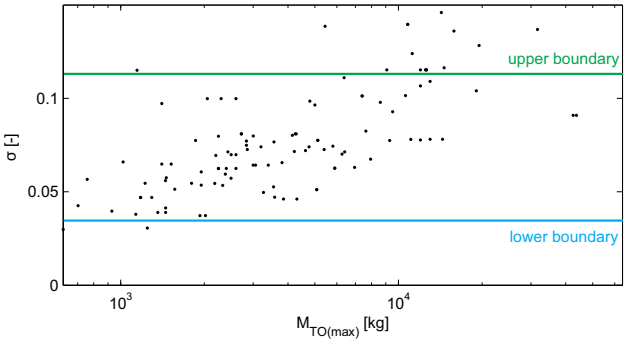


FIG 18. Rotor solidity from helicopter database

- **Blade Loading**

Blade loading is derived from division of the thrust coefficient by the rotor solidity, describing the aerodynamic workload of each blade:

(11) $$C_T/\sigma = \frac{s \cdot M_{TO}\, g}{\varrho\, c\, N_b\, R\, U^2}$$

To address the multirotor configurations properly the trust sharing coefficient is introduced. At equal thrust sharing of two rotors it would be 0.5. But both the tandem and coaxial arrangement have one rotor, which produces more than 50% of the take-off mass thrust, so the coefficient is set to 0.6, as it corresponds to the results by Bourtsev et al. from [15].

In FIG 19 it can be seen that the majority of the helicopters throughout the weight classes is set for a value of somewhere between 0.07 and 0.10 (in hover). The maximum value of the blade loading in the design loop should not exceed 0.12 as it is considered as boundary value for rotor stall [16].

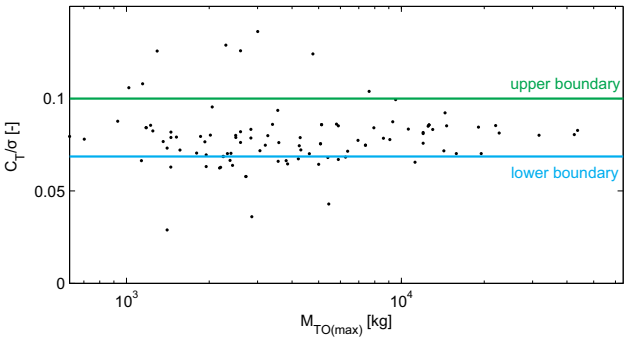


FIG 19. Blade loading from helicopter database

- **Blade Tip Speed**

The blade tip speed has also an almost universal character, varying between values of 180 m/s and 220 m/s (FIG 20). Even though there are many successful designs with speeds of 150 m/s but mostly only with light and ultra-light designs, which are not designed for the speed of more than 200 km/h and therefore do not exceed high advance ratios either.

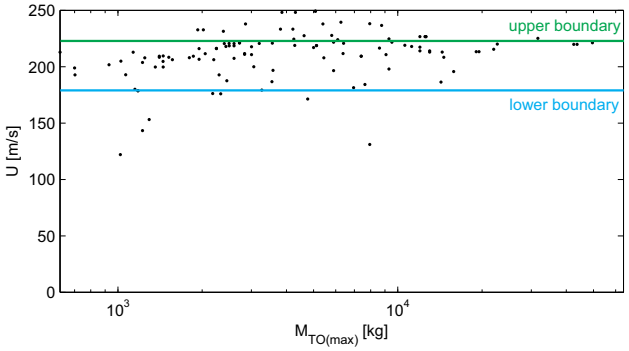


FIG 20. Blade tip speed from helicopter database

- **Mach Number at Cruising Speed**

The Mach number at cruising speed is determined by the set up blade tip speed:

$$Ma_c = \frac{(V_c + U)}{a} \quad (12)$$

In most cases a value of 0.85 can be defined as good target value for the design, as values above cohere with high profile drag at the advancing blade side and therefore high power consumption and vibrations. In FIG 21 it can be seen that there is only a thin margin of values where the majority of the designs is spread.

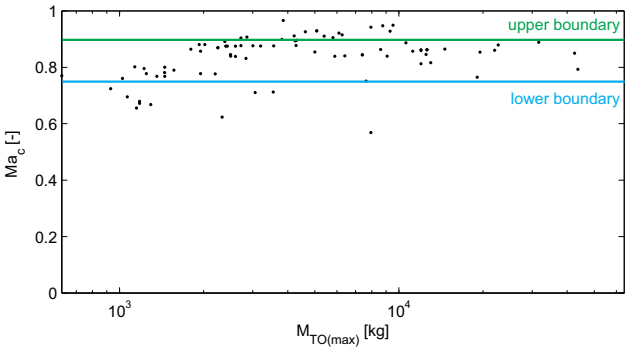


FIG 21. Mach number at blade tip from helicopter database

- **Advance Ratio at Cruising Speed**

The advance ratio at cruising speed is the rival parameter to the Mach number as the blade tip speed is in the denominator of the equation:

$$\mu_c = \frac{V_c}{U} \quad (13)$$

In most cases a value of 0.3 can be defined as good target value for the design at cruising speed to have some speed reserves. The advance ratio can be seen as a soft border, compared to the Mach tip speeds. Though high values cohere with high vibration levels as it describes the diameter of a circle of reversed flow on the retreating blade side of the rotor disc. In FIG 22 it can be seen that the majority margin is between 0.25 and 0.4.

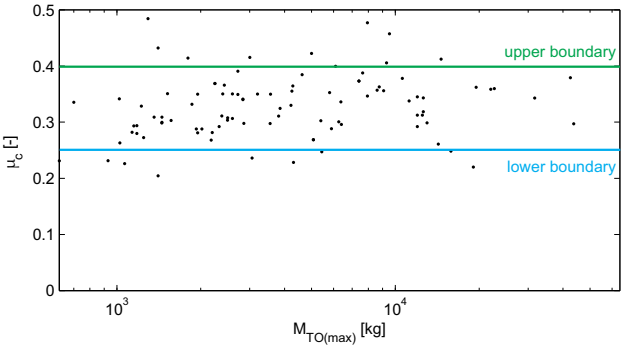


FIG 22. Advance ratios from helicopter database

- **Lock Number**

The Lock number is an important parameter characterizing the flapping behavior of the rotor blade:

$$\gamma = \frac{\varrho\, c_{l_\alpha} c\, R^4}{I_b} \quad (14)$$

It represents the ratio of the aerodynamic and inertial forces acting on the blade. Lower values of the Lock number are associated with a high (and in most cases preferred) inertial characteristic of the blade, as the flapping moment of inertia is in the denominator of the equation.

In FIG 23 there is only a selection of the database shown, as the data concerning the blade masses and the moments of inertia are more difficult to acquire or simply not published.

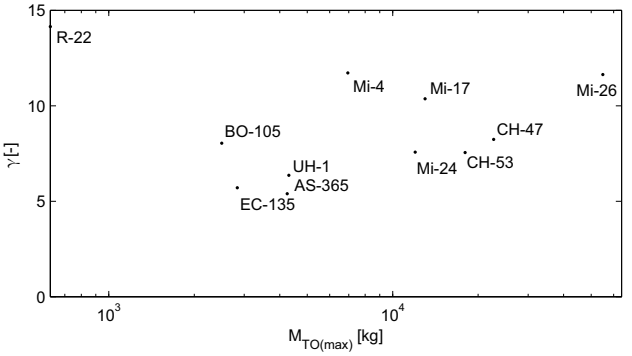


FIG 23. Lock Number from reduced helicopter database

Nevertheless, the Lock numbers are found to have values between 5 and 12, larger with increasing take-off masses.

- **Energy Ratio**

Another parameter concerning the responses of the rotor optimization focuses on the autorotational behavior of the helicopter. The main idea behind this is to consider the kinetic energy of the rotor(s) at nominal rotor speed related to the translational kinetic energy of the helicopter as a whole in vertical autorotation.

$$\varepsilon = \frac{E_{rot}}{E_{trans}} = \frac{1/2 \cdot N_r \cdot N_b \cdot I_b \cdot \Omega^2}{1/2 \cdot M_{TO}\, w_d^2} \quad (15)$$

The vertical descent velocity at ideal autorotation can be estimated as 1.8 times the induced velocity in hover [16]:

(16) $$w_d = 1.8 \cdot v_i = 1.8 \cdot \sqrt{\frac{M_{TO} \cdot g}{2 \cdot \varrho \cdot \kappa_{ov} \cdot \pi \cdot R^2}}$$

The overlapping factor for two rotors configurations is calculated from Johnson [16] to:

(17) $$\kappa_{ov} = \sqrt{\frac{2}{2-m}}$$

For the coaxial rotor arrangement the value of m is 1 and hence the overlapping factor is the square root of 2. For the tandem arrangement the factor is a function of the rotor shaft spacing:

(18) $$m = \frac{2}{\pi}\left[\arccos\left(\frac{l}{2R}\right) - \frac{l}{2R}\sqrt{1-\left(\frac{l}{2R}\right)^2}\right]$$

With these formulas equation (15) becomes:

(19) $$\varepsilon = \frac{E_{rot}}{E_{trans}} = \frac{N_r \cdot N_b \cdot I_b \cdot \Omega^2}{1.62 \cdot \frac{M_{TO}^2 \cdot g}{\varrho \cdot \kappa_{ov} \cdot \pi \cdot R^2}}$$

In FIG 24 the energy ratio values are shown for the same reduced database.

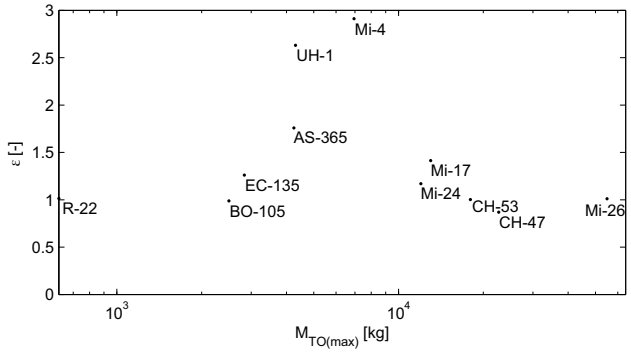


FIG 24. Energy ratio from reduced helicopter database

It can be seen that the energy ratios of the selected database start at values of 1. Helicopters with known as "good at autorotations"-behavior such as UH-1 and Mi-4 exhibit values above 2 and representatives of the "bad at autorotations"-behavior such as the light R-22 hold values of 1. With a high energy ratio (above 2) it is possible that the helicopter should be able to perform a horizontal autorotational descent to the ground. With a value of 1 this is not feasible, because it is impossible to use the entire rotational energy for the complete deceleration of the descending helicopter. The rotor thrust breaks down due to stall at 60-70% of the nominal rotor speed [16].

- **Blade Mass Density**

The last parameter concerning the rotor design and optimization is the blade mass density, which is also analyzed from the (reduced) helicopter database.

The parametrization of the blade geometry follows a simple approach considering the relative blade thickness as constant:

(20) $$\delta_b = \frac{d}{c} \approx 0.12$$

The area ratio of the profiled section is usually a function of the relative thickness, but can be assumed constant to:

(21) $$\bar{A}_b = \frac{A_b}{\delta_b \cdot c^2} \approx 0.7$$

The mass distribution of the blade is then:

(22) $$m_b = \delta_b \cdot c^2 \cdot \bar{A}_b \cdot \varrho_b$$

With it, the blade mass is calculated to:

(23) $$M_b = m_b \cdot R$$

The moment of inertia of each blade with a correction factor of 1.1 (to fit the moments of inertia in the database) due to non-uniformity of the blade mass distribution becomes:

(24) $$I_b = \frac{1}{3} M_b \cdot (1.1 \cdot R)^2$$

The last equations were applied on the (reduced) helicopter database to get an insight on the blade mass density trend. In FIG 25 it can be seen that the density is very high for the shown light helicopters, continuously decreasing to almost one third of the heaviest Mi-26, compared to the maximum value of the R-22. For the rotor optimization the density between the upper and lower best fit curves is used.

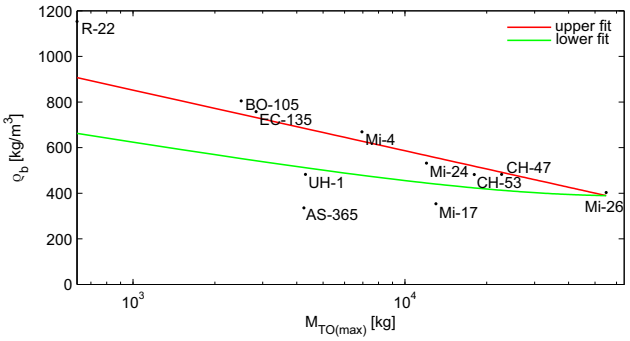


FIG 25. Blade mass density from the reduced helicopter database

### 3.7. Blade Twist

The blade twist of the rotor is optimized for the lowest required power needed at the required speed. The only restriction is that the collective blade angle may not exceed 20° (to not further decrease the effectiveness of the rotor at hover, since the inner sections of the blade will get into the overpitched stall).

After the first successful rotor optimization loop the rotor masses and with it the take-off mass changed. So the whole design is handled back to the 1st station of the design loop again. In that case the re-calculation of the fuselage mass, as the geometry of the fuselage due to rotor parametrization changed as well.

The 2nd station is the re-calculation of the fuselage aerodynamics.

The 3rd station is the power source estimation and consequent refilling to fulfill the unchanged requirements from the initialization.

The 4th station is the 2nd entry into the rotor optimization loop, and so on.

## 4. RESULTS

In the project EDEN the design loop and its components are constantly improved with the aim to achieve the ability to perform preliminary design not only for the 3 main helicopter types, but also for their derivates into compound helicopters.

To demonstrate the interim abilities of the design loop the following helicopters from three configurational types were subjected to a “re-design”:

- Mil’s Mi-8
- Kamov’s Ka-226
- Boing Vertol’s BV-107 (known as CH-46)

From each helicopter the known data of payload capacity, cruising speed and the corresponding range were used as TLARs for the EDEN design loop. All helicopters were subjected to the same boundary conditions within the rotor optimization process. In FIG 26 the rotor optimization of the Mi-8 is shown as overall time history.

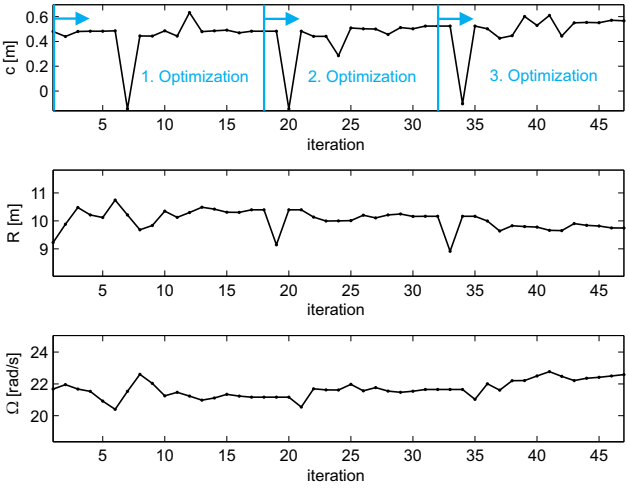


FIG 26. Rotor optimization process of the Mi-8 re-design

Comparing the initial with the final values, it can be seen that every parameter increased. The main changes were made in the first optimization call (until 17th iteration). The radius increased up to 11 meters, the rotor frequency had the tendency to compensate it, regarding all the boundary margins. The algorithm also tried negative values for the chord (which cannot be prevented, due to the search for a global optimization goal), but instantly returned back. Comparing the following 2 calls with the first, it can be seen that all parameters had a more relaxed behavior.

The re-design results of all three helicopters compared to the original values are shown in FIG 27 and the results of the masses and installed power in FIG 28. One of the striking results is the blade tip speed, which hit the upper boundary of 220 m/s. The blade radius of the Mi-8 was reduced by 10%, the chord is increased by almost the same factor. All other rotor characteristics are very close to the original values. The resulting take-off mass is almost identical to the original value, the empty mass now is 2% higher. The needed fuel mass is almost 15% below the original value, so is the installed power, indicating less parasite drag than the original.

The results of the multirotor configurations had reached almost the maximum set blade loading of 0.1 with the maximum tip speed of 220 m/s. The main difference and hence influence on the rotor optimization of the multirotor configurations was found for the deviation of the empty mass compared to the originals – the re-design became 16-28% lighter. With it, the required power and the needed fuel mass also dropped below the original values.

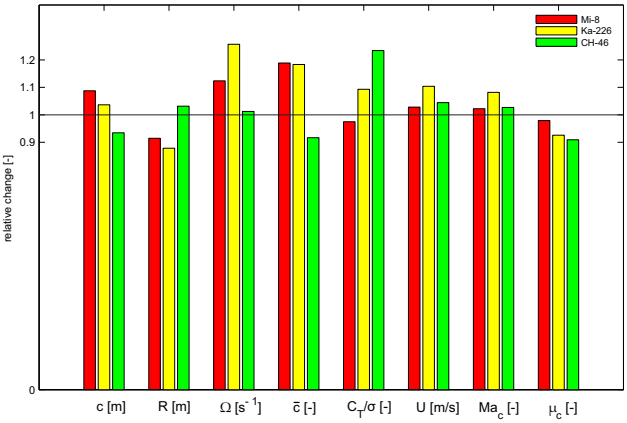


FIG 27. Rotor optimization results of the re-design

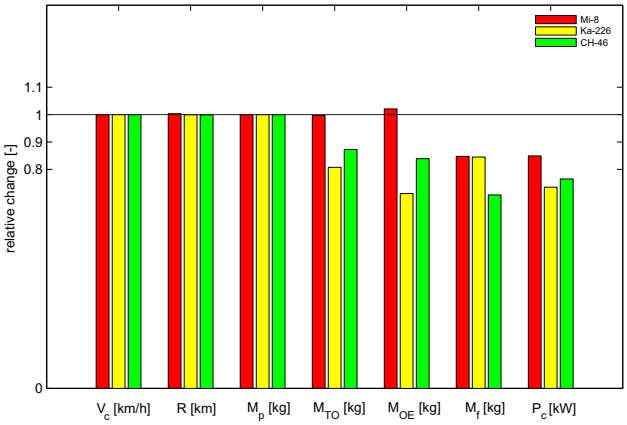


FIG 28. Mass and performance results of the re-design

## 5. CONCLUSION AND OUTLOOK

The objective of the project EDEN is a generic design of a rotorcraft according to a given set of TLARs. It has been demonstrated that different configurations were designed for a given minimal set of mission relevant requirements. In general it can be concluded that the rotor optimization presented here finds very reasonable parameter sets, even with wide margin boundary conditions.

- The porting to the DLR’s software framework RCE including the networking of the three institutes was achieved and nearly all tools are reintegrated.
- On the basis of the new framework an iterative design loop was created, which includes the rotor optimization loop.
- A concept for the generic helicopter design for different configurations was developed and implemented.

The design loop itself showed good results, but the main difficulty is the estimation of the operating empty mass and the estimation of the aerodynamic drag, which in turn results in underestimation of the installed power and less required fuel mass. Following steps have to be performed in the near future:

- The prediction of the operation empty mass (for unconventional configurations) has to be improved.
- The full integration of the generic structural design including the FEM analysis has to be completed.
- Improvement of overall drag prediction methods.

## 6. REFERENCES


[1] D. P. Raymer, "*Aircraft Design: A Conceptual Approach"*, Reston, VA, American Institute of Aeronautics and Astronautics, 2006.

[2] L. Nicolai and G. Carichner, "*Fundamentals of Aircraft and Airship Design, Volume 1"*, Reston, VA, American Institute of Aeronautics and Astronautics, 2010.

[3] D. M. Layton, "Introduction to Helicopter Design", AIAA Professional Studies Series, Salinas, CA, 1992.

[4] J. Roskam, "*Airplane Design",* Lawrence, KS, Design, Analysis and Research Corporation (DARcorporation), 1985.

[5] W. Johnson, *"NDARC - NASA Design and Analysis of RotorCraf,"*, Moffett Field, CA, 2009.

[6] J.-F. Boer and J. Stevens, *"Helicopter Life Cycle Cost reduction through pre-design optimisation"*, 32nd European Rotorcraft Forum, 12-14 September 2006.

[7] A. Khalid and D. P. Schrage, *"Helicopter Design Cost Minimization using Multidisciplinary Design Optimization"*, 63rd Annual Forum and Technology Display of the American Helicopter Society, May 1-3, 2007.

[8] P. Basset, A. Tremolet, F. Cuzieux, C. Schulte, D. Tristrant, T. Lefebvre, G. Reboul, F. Richez, S. Burguburu, D. Petot, and B. Paluch, *"The C.R.E.A.T.I.O.N. project for rotorcraft concepts evaluation : The first steps"*, 37th European Rotorcraft Forum, September 13-15, 2011.

[9] M. N. Beltramo and M. A. Morris*, "Parametric study of helicopter aircraft systems costs and weights"*, Hampton, VA, 1980.

[10] R. W. Prouty, "*Helicopter Performance, Stabililty, and Contro",* Malabar, FL, Krieger Publishing Company, 1990.

[11] D. Palasis, *"Erstellung eines Vorentwurfsverfahrens für Hubschrauber mit einer Erweiterung für das Kipprotorflugzeug"*, Düsseldorf, 1992.

[12] P. Kunze, *"Parametric Fuselage Geometry Generation and Aerodynamic Performance Prediction in Preliminary Rotorcraft Design"*, 39th European Rotorcraft Forum, 2013.

[13] B. Maskew, *"Program VSAERO theory document - NASA CR-4023"*, Redmond, WA, 1987.

[14] M. J. D. Powell, *"A view of algorithms for optimization without derivatives"*, Cambridge, UK, 2007.

[15] Bourtsev, B.N., Ryabov, V.I., Selemenev, S.V., Butov,V.P. *"Helicopter Wake Form Visualization Results and their Application to Coaxial Rotor Analysis in Hover"*, 27th European Rotorcraft Forum, Moscow, Russia, September 11-14, 2001.

[16] Johnson, W., *"Rotorcraft Aeromechanics"*, Cambridge University Press, 2013.